SO 2 deactivation mechanism of NO oxidation and regeneration of the LaCoO 3 perovskite

Ferenc Martinovic, Quang Nguyen Tran, Fabio Alessandro Deorsola, Samir Bensaid, Regina Palkovits, Werner Paulus, Barbara Bonelli, Francesco Di Renzo, Raffaele Pirone

SO2 deactivation mechanism of NO oxidation and regeneration of the LaCoO3 perovskite

Ferenc Martinovic,[a,b] Quang Nguyen Tran,[a,c] Fabio Alessandro Deorsola,[*a] Samir Bensaid,[a] Regina Palkovits,[b] Werner Paulus,[c] Barbara Bonelli,[a] Francesco Di Renzo[c] and Raffaele Pirone[a]
a.Politecnico di Torino, Department of Applied Science and Technology, Corso Duca degli Abruzzi 24, 10129 Torino, Italy.
b.Institut für Technische und Makromolekulare Chemie, RWTH Aachen University, Worringerweg 2, 52074 Aachen, Germany.
c. Institut Charles Gerhardt, Université de Montpellier-CNRS-ENSCM, Place Eugène Bataillon, 34095 Montpellier, France.

Electronic Supplementary Information (ESI) available: See DOI: 10.1039/C9CY02478F

The deactivation mechanism and methods to cope with the poisoning by SO2 of LaCoO3 perovskite-based NO oxidation catalyst were investigated. The LaCoO3 perovskite was synthesized by a sol-gel method and the fresh, sulphate-deactivated and regenerated catalysts were characterized by X-ray Diffraction, X-ray Photoelectron Spectroscopy, H2- and soot-Temperature Programmed Reduction, Temperature Programmed Desorption and Diffuse Reflectance Infrared Fourier Transform Spectroscopy. The SO2 poisoning strongly affected the NO oxidation activity. It was demonstrated that the deactivation mechanism proceeds in two stages: initially the active sites with basic character are blocked by SO3 and subsequently the lanthanum sulphate salts grow progressively on the surface and cobalt is unaffected. Above 500 °C, the surface bound sulphates become mobile and migrate into the bulk of the catalyst. Several prevention and regeneration methods were proposed and tested. By mixing the catalyst with Ca(OH)2 as an adsorbent nearly 50% of the original activity was retained. Regeneration by diesel soot was presented here for the first time, where the blocking oxygen can spill over to the soot oxidizing it and releasing the bound sulphur as SO2 and CO2. Furthermore, a facile regeneration method was explored by washing the deactivated catalyst to dissolve the small amounts of sulphates on the surface.

Introduction

Perovskite structured materials are an interesting type of catalysts due to their tunable catalytic activity, thermal stability and peculiar redox properties.[1] In the automotive exhaust treatment, they have been suggested as a potential low-cost substitute for the platinum group metals Pt-Pd (PGM) widely used in three way catalysts, diesel oxidation catalysts (DOC), catalysed diesel particulate filters (cDPF) and lean NOx traps (LNT).[1–7] The most promising perovskites are lanthanides with LaBO3 structure, where B is usually Fe, Mn and Co in the +3 oxidation state. Out of these three, LaCoO3 has shown the highest activity in the automotive application, partly due to its interaction and high oxidation ability of NOx.[1–6] Despite advances made in hydrodesulphurization, deep removal to produce low sulphur concentration in fuel (<10 ppm) remains a challenge. Hence, sulphur-based compounds are invariably present in the fuel and produce SO2 during combustion. In different degrees, SO2 represents a poison to almost all catalysts used in aftertreatment systems. The most sensitive to sulphur are catalysts that are characterized by an alkaline surface (e.g. barium in LNT), which can form stable sulphates and deactivate the catalyst active site. While there are many detailed studies of SO2 poisoning and deactivation on Pt-Ba based LNT systems,[8–10] only few and conflicting reports are available on the deactivation of the perovskite-based catalysts.[11–19]

The reason is that, in the deactivation studies, the applied reaction conditions are drastically different, depending on the application and/or the aims of the study. For example, in studies concerning the hydrocarbon catalytic oxidation at high temperature (>500 °C) the main results showed that sulphur diffuses in the bulk of the perovskite structure,13,15,20 whereas studies made at lower temperature concluded that the sulphur insertion was limited and the deactivation was mainly a surface phenomenon.[11,14,17] The point at which all agree is the competition for the same catalytic cycle and competition of SO3 and NO2 for the same active site characterized by alkaline character. The first goal of this work is to unravel the deactivation mechanism of NO oxidation by SO2 under relevant reaction conditions that typically occur in diesel exhaust aftertreatment system. The second goal of the work focuses on alternative methods of SO2 poisoning management. The typical methods suggested for the regeneration of sulphur poisoned LNT catalysts involve the injection of large amounts of reductant (such as H2, C3H6, NH3) and high regeneration temperatures (>600 °C), which result in high fuel penalty and catalyst damage.[9–11] Based on the deactivation mechanism and different chemical nature of the perovskite-based catalysts compared to the PGM based LNT, several novel methods are suggested:

1. Use of inexpensive Ca(OH)2 as SO2 adsorbent and bed guard.
2. Use of soot for enhancing the release of SO2. Soot is a pollutant abundant on the cDPF, which is one of the main catalytic potential applications of LaCoO3.
3. Facile regeneration at room temperature, by washing with distilled water.

In this work all three alternative regeneration methods are investigated and discussed.

Experimental procedures

Catalyst preparation. The LaCoO3 catalyst was prepared by following the citrate sol-gel method. Proper equimolar amounts of La(NO3)3·6H2O and Co(NO3)2·6H2O (each 5 mmol) were dissolved in 60 mL of deionized water. 20 mmol citric acid monohydrate was added under stirring to the mixture and the pH adjusted to 7 by adding ammonia solution (10% v/v). The solution was heated to 80 °C and evaporated under stirring. As the liquid volume decreased, the chelated metallic ions were crosslinked by citric acid and the viscosity increased. The as-obtained gel was dried at 110 °C for 24 hours after which it was crushed and pre-calcined at 350 °C for 1 hour to decompose the citric acid. The obtained powder was ground in a mortar and calcined at 700 °C for 6 hours (5 °C/min heating rate).

Regeneration of the poisoned samples was made by placing the sulphated LaCoO3 (LaCoO3-S) in 20 mL of distilled water and by adjusting the pH to 7 by adding ammonia solution. The samples could be also regenerated by using distilled water without adjusting the pH; the ammonia solution was added only to avoid metal leaching and potential sample loss. The slurry was stirred for 30 min at room temperature, after which it was separated by centrifugation. The regenerated sample was dried at 200 °C for 12 h and tested again.

Several successive deactivation-regeneration cycles were conducted, and the so obtained samples were referred to as LaCoO3-R followed by a number indicating the number of regeneration cycles. A total of 5 poisoning-reactivation cycles was reached.

Catalyst characterization. X-ray diffraction were recorded on a Philips PW 3040 X'Pert instrument with Cu anode for the Kα generation at 40 kV operating voltage. A pixel array detector enabled continuous data acquisition in the 2θ range 20-80°, with a step of 0.013°. The cell parameters and the crystallite sizes were evaluated by Rietveld refinement. The specific surface area was determined by N2 physisorption at -196 °C on Micrometrics Tristar 3020 instrument.

Before the analysis, the samples were evacuated at 200 °C for 2 hours. The reported specific surface area was calculated according to the BET method.
X-ray photoelectron spectroscopy (XPS) was performed in a PHI Versaprobe apparatus, using Al Kα radiation with band-pass energy of 187.85 eV and 23.5 eV for the high-resolution scan, a 45° take off angle and a 100.0 μm diameter X-ray spot size. The lines of La, Co, O and S were detected. To observe the depth profile and the deactivation mechanism, the deactivated LaCoO3-S was sputtered with Ar+ gun to remove the top layer and the XPS analysis was repeated afterwards.
The hydrogen temperature programmed reduction (H2-TPR) was performed on a ThermoScientific TPRDO 1100 instrument equipped with a thermal conductivity detector (TCD) detector. In a typical experiment, the catalyst was pre-treated in-situ under inert flow of Ar at 500 °C for 1 hour to remove any adsorbed species. Afterwards, the sample was cooled down and 20 mL/min of a gas mixture of 5% H2 in Ar was flown over 60 mg of the sample with a 5°C/min rate of temperature increase until 900 °C. The H2-TPR profile for the poisoned LaCoO3-S sample was also repeated in the experimental setup described below, to detect by means of mass spectrometer the various potential species formed during reduction. The soot-TPR, H2-TPR and temperature programmed desorption (TPD) of the poisoned sample was performed in a slightly different set-up, with the outlet connected to a mass spectrometer to follow the evolution of all the potential species. Typically, 60 mg of sample (LaCoO3 and LaCoO3-S) was used under 60 mL/min Ar flow and 5 °C/min heating rate. For the soot-TPR the fresh and poisoned catalyst was mixed with soot in a planetary ball mill in 10: 1 catalyst: soot mass ratio.
Morphology and elemental composition were determined by field emission scanning electron microscopy-Energy-dispersive X-ray spectroscopy (FESEM-EDS) under high vacuum, using Zeiss MERLIN Gemini II equipped with EDS at 3 keV accelerating voltage and different magnifications.
Diffuse Reflectance Infrared Fourier Transform Spectroscopy (DRIFTS) analysis was performed on Vertex-70 IR spectrometer equipped with Praying Mantis (Harrick) heated reaction cell. The samples LaCoO3 or LaCoO3-S were mixed to KBr in 100:2 mass ratio. The so-prepared samples were placed into an isolated cell and kept under inert N2 flow during the test. LaCoO3-S was heated to 400 °C, 500 °C, 550 °C and 600 °C and held at constant temperature for 30 min after which they were quenched at 200 °C/min cooling rate. All the IR spectra were collected in absorbance mode at 30 °C (2 cm^{-1} resolution; 64 scans; wavenumber range 1800-800 cm-1).
Catalytic tests. The catalytic tests were conducted in a glass tube reactor with i.d. 10 mm. The catalyst was placed on a glass membrane inside the reactor and heated in an isolated vertical furnace with a thermocouple in the catalytic bed for programmable heating. The outlet was connected to ABB Limas and Uras nondispersive infrared and ultraviolet (NDIR and UV) analysers for continuous measurement of CO, CO2, NO, NO2.
The deactivation was performed by flowing 600 mL/min of 60 ppm SO2, 500 ppm NO, 4% O2 in N2 over 200 mg of catalyst. To prepare the LaCoO3-S sample, the deactivation was performed at constant temperature of 300 °C as it is a typical temperature found in diesel exhaust. Deactivation was considered complete when the NO oxidation rate dropped to 0, i.e. the NO2/NOx ratio after the catalytic bed was the same as at the inlet. The poisoning time typically lasted 90 minutes.
To demonstrate the effectiveness of an adsorbent towards the SO2 management, 200 mg of LaCoO3 was mixed with 100 mg of Ca(OH)2 before performing the deactivation, under the same conditions described before, at 300 °C and also at 500 °C. Different adsorbent catalyst configurations were investigated and compared:
1) LaCoO3 and Ca(OH)2 gently mixed with spatula to obtain “loose contact”;

2) LaCoO3 and Ca(OH)2 mixed in planetary ball mill for 15 minutes to obtain “tight contact”;
3) Zoned dual-layer configuration whereby the LaCoO3 bed was located downstream of the Ca(OH)2 bed.

To show competitive adsorption of NOx and SO2, the catalyst was first saturated with NOx at 200 °C. When the NOx concentration was stable, NOx flow was switched off and the catalyst purged with N2 to remove weakly adsorbed NOx. Once the NOx concentration in the gas phase decreased to 0, 60 ppm of SO2 in 4% O2 and N2 was introduced to the reactor and the desorbed NOx species were measured. During the whole test, the temperature was kept constant at 200 °C.

NO oxidation tests were made under the aforementioned conditions, without SO2 in the feed stream and at constant heating rate of 5 °C/min in the temperature range 150-600 °C. The NO oxidation performance of the fresh catalyst was compared to that of the regenerated LaCoO3-R.

Results and discussion

Characterization results.

The XR-diffractograms of the samples LaCoO3, LaCoO3-S and LaCoO3-R5 are presented in Figure 1. In all the samples, only the LaCoO3 perovskite phase is detected without any Co3O4 or La2O3 phases, indicating good crystallization of the sample and the perovskite formation. The cell parameters of the rhombohedral perovskite structure (a = 5.441(5) and c = 13.10(5)) are not significantly affected by the treatments. The degree of crystallinity is the same with all the samples, as even after 5 regeneration cycles the normalized peak intensities are the same. The value of crystallite size as calculated by the Williamson-Hall method is 41 nm for the parent LaCoO3 sample, decreases to 32 nm for LaCoO3-S and stabilizes to 28 nm for regenerated samples from LaCoO3-R1 to LaCoO3-R5. The main diffraction peaks of La2(SO4)3, Co2O3, orthorhombic La2O3 and cubic La2O3 (expected at the 2θ values 28.33°, 36.56°, 29.92° and 33.19° respectively) were not detected by XRD (25-30° magnified in Figure 1).

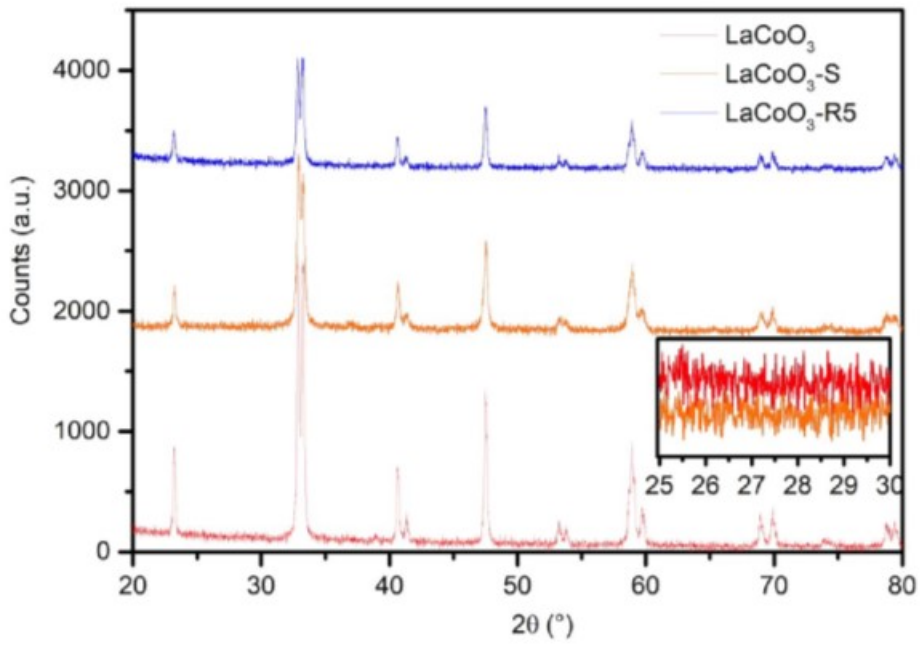

Fig. 1 Powder XRD diffractograms of the LaCoO3, LaCoO3-S and LaCoO3-R5 catalysts.

Conversely several reports,[15,16,20] show the presence of peaks of La2(SO4)3 as a result of SO2 poisoning. The major difference is that for those, the deactivation by SO2 was made at much higher temperature, well above 500 °C, and under different reaction conditions. At high temperature, changes in the perovskite structure can occur more readily and sulphates can diffuse into the bulk by forming a mixed phase. Here the deactivation proceeded at 300 °C (lower temperature) through a different mechanism and, as will be discussed later on, sulphates formed only at the surface, without affecting the crystalline structure of the perovskite. In fact, no changes in both the symmetry and lattice parameters were observed for LaCoO3, LaCoO3-S and LaCoO3-R5. As the total quantity of Sulphur was low and dispersed uniformly on the surface in a nm thin layer (vide infra), the sulphate containing phases could not be detected by XRD. The decrease of crystallite size, as observed by XRD linewidth, is not contradictory with the stability of grain size as observed by FE-SEM. As the decrease in crystallite size is mainly observed after the first catalytic use of the material, it seems likely that the largest grains have been fractured by thermal stress without physical separation of the formed sub-grains, hence with no changes of grain morphology.

The particles had a globular shape and were interlinked, forming regular intergranular macropores. The FE-SEM analysis (Figure S1) showed powders with a morphology typical of perovskites synthesized by the citrate complexation method. Both the LaCoO3-S and the LaCoO3-R5 catalysts presented no significant difference in the morphology as compared to the fresh catalyst (Figure S1). No significant difference in the BET specific surface area was observed as well, the corresponding values being 12.6, 12.5, 9.1 m2/g for the LaCoO3, LaCoO3-S and LaCoO3-R5 catalysts, respectively. The slight decrease of specific surface area could be attributed to the filling of the some intergranular spaces by smaller particles (most likely La(OH)3) that formed during the dissolution process. Conversely, significant decrease of the specific surface area was reported after deactivation by SO2 albeit in different reaction conditions,[15,16,20] i.e. when the deactivation was made at high temperature (500-600 °C) for prolonged periods with catalysts calcined at lower temperature than in this study. In those cases, the decrease in the specific surface area could be attributable, at least partially, to thermal sintering during sulphation. In this work, instead, the calcination temperature was 700 °C and the sulphation temperature 300 °C and thus, the specific surface area was stabilized during the calcination and no significant decrease in the surface area was observed due to thermal effect, nor due to sulphation.

The total consumption of H2 during H2-TPR was 6.2 mmol/g for both the parent LaCoO3 and the regenerated LaCoO3-R5 (Figure 2). This amount corresponds to the stochiometric reduction of Co3+ to metallic Co via the reduction steps: Co3+ → Co2+ → Co0.21 It is generally accepted that the reduction of LaCoO3 perovskites occurs along the reactions R1-2. This can explain the occurrence of two clearly separated reduction steps, at variance with the reduction of Co3O4 that has only a single peak in the low temperature region.[22] The reduction peak between 200-450 °C corresponds to the reduction of Co3+ to Co2+ (reaction R1).[21] This first reduction step can be separated into several components, showing two distinct reduction temperatures at 325 and 400 °C. This is most likely due to the inhomogeneity and the presence of different types of Co3+ and O2- species in the sample. The second peak between 550-650 °C is due to the reduction of Co2+ to metallic Co0 with the consequent loss of the perovskite crystalline phase and the formation of Co/La2O3 system. Indeed, as expected, the H2 consumption corresponding to the second peak of LaCoO3 and LaCoO3-R5 TPR profiles is twice the H2 consumption of first peak. In contrast, the LaCoO3-S sample did not show any H2 consumption at ow temperature, in that the first peak was absent and reduction started only at 400°C meaning that the Co3+ to Co2+ reduction is deactivated.

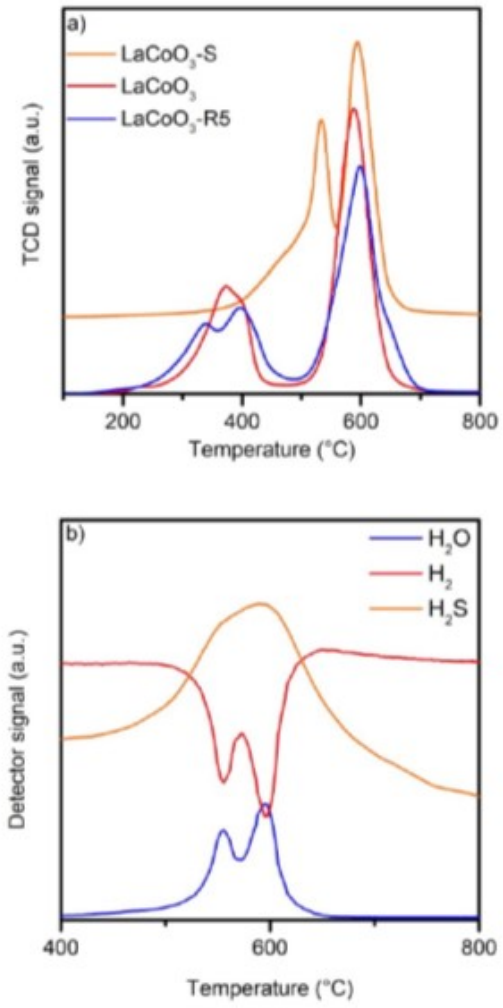

Fig. 2 a) H2 consumption during H2-TPR, b) H2S and H2O evolution during the reduction of LaCoO3-S.

The adsorbed sulphates had to be removed first by reducing them to H2S (Figure 2b), before both the lattice and surface oxygen of perovskite could be accessible for the subsequent reduction with H2. Interestingly, not all the sulphates had to be removed before the reduction could start, as the H2S and the H2 consumption initiated concurrently. The availability of redox sites for H2 reduction was dependent on the surface coverage and as more of the sulphates were removed, the H2 consumption increased and full reduction was achieved sooner, as shown in Figure 2b. At 600 °C only 50% of the H2S was released, while most of the catalyst was reduced.
This provides evidence that the redox sites are blocked by strongly bound sulphates and the reactive oxygen species active for NO oxidation are inactivated. Only after the surface sulphate removal the reduction proceeds.

(R1) 2 LaCoO3 + H2 → 2 LaCoO2.5 + H2O R1 (200-420 °C)
(R2) 2 LaCoO2.5 + 2 H2 → 2Co + La2O3 + 2 H2O R2 (500-650 °C)
(R3) LaCoO3-xSO3 + 4xH2 → LaCoO3 + H2O + xH2S R3 (500-650 °C)

Figure 3 reports the XP-spectra concerning LaCoO3, LaCoO3-S, and LaCoO3-R5 samples. The O 1s XP spectra shows a marked increase in the poisoned sample of the peak at 532 eV which corresponds to the characteristic electronic state of oxygen in sulphate form, originating from the $SO4^{2-}$ oxygen.[15,23] Further evidence of surface sulphates comes from the S2p peak as the band centred at 169 eV is a clear indicator for S in the $SO4^{2-}$ (i.e. S^{6+}) form.[23] The XPS analysis in the Co 2p binding energy region indicates that cobalt is present as Co^{3+} as its characteristic peaks are identified at 780 eV and 795 eV.[23] The lack of satellite peaks at 785 eV and at 803 eV allows excluding the occurrence of Co^{2+} species in the samples, in agreement with the H^{2-} TPR results. The XPS analysis of the poisoned sample does not indicate any change in the Co XP spectra and the characteristic peak assignable to cobalt sulphate, expected at 784 eV, is missing.[23] The La 3d XP spectra, in contrast, showed a clear transformation in the poisoned sample since La in the sulphate form was also detected besides the characteristic spectra of the oxide form found in the perovskite. The multiplet splitting in the La 3d3/2 and 3d5/2 regions of the LaCoO3 presented a ΔE of 4.1 and 5.1 eV which is characteristic of La in the oxide form.21,23 After poisoning, the resulting spectra was a combination of the oxide and sulphate form which features a lower ΔE of 3.5 eV. The combination of these two forms were difficult to deconvolute unambiguously as the

characteristic positions are only slightly shifted (difference of 0.15 eV) and significantly overlapping.
Sputtering with an Ar+ ion gun was used to remove ca. 30 nm surface layer from the LaCoO3-S sample. The XP spectra taken after sputtering showed the same features of the fresh sample (not shown) and the absence of S, confirming that SO2 poisoning mainly affected the surface rather than the bulk after the deactivation was performed at 300 °C.

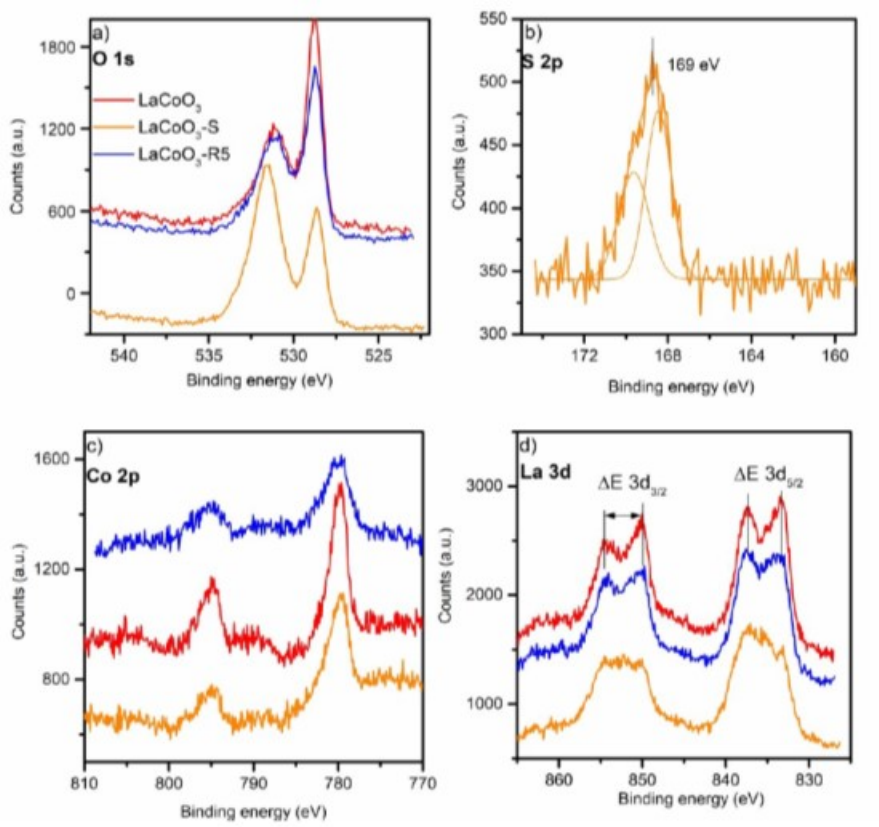

Fig. 3 XPS spectra of a) O 1s, b) S 2p, c) Co 2p and d) La 3d band of the fresh, poisoned and regenerated by washing samples.

The La/Co and S/La atomic ratios of the samples in the bulk (determined by EDS) and at the surface (XPS) are compared in Table 1. The surface S/La ratio increases to 0.4 and, correspondingly, the La/Co ratio also increases, confirming the formation of lanthanum sulphate. This likely leads to the modification of the perovskite structure due to the reaction of La with S. The reported chemical analysis allows estimating ca. 1 wt% of sulphur in the bulk. However, the surface S/La ratio equals 0.4, i.e. a much lower than the expected 1.5 ratio expected for the complete transformation into La2(SO4)3.

Table 1 XPS and EDS analysis of the surface and bulk characteristics of the presented samples.

	La/Co		S/La	
	Total	Surface	Total	Surface
$LaCoO_3$	1	1.1	-	-
$LaCoO_3$-S	1	1.25	0.085	0.4
$LaCoO_3$-R5	1	1.1	-	-
After sputtering	1	2.15	0	0

The difference between the bulk and surface sulphur contents point out that the sulphate formation is likely restricted to few surface monolayers (~5 nm) at the surface when poisoning occurs at 300 °C. The poisoning is also accompanied by the enrichment of the surface by La relative to Co to La/Co 1.25 from 1.1. This provides further confirmation of the previous results that the sulphates are restricted to the surface and they are bound to the A and not the B site in the ABO3 perovskite. It should be noted that the high La/Co ratio (2.15) after sputtering is most likely the consequence of the preferential ejection of the lighter Co (A = 58.93) with respect to the La (A = 138.91) during the ion sputtering, rather than a change in the chemical composition of the perovskite.
Figure 4 reports the DRIFT spectra of the LaCoO3 and LaCoO3-S samples collected at room temperature after heating at 300, 400, 500, 550 and 600 °C to induce sulphate migration. The LaCoO3-S at 300 °C presents two sulphate peaks at 990 and 1383 cm-1 and a broad band centred around 1130 cm-1, likely a combination of a multitude of different vibration modes of amorphous sulphates differently bound to the surface, most commonly ascribed to bidentate sulphates.11,24

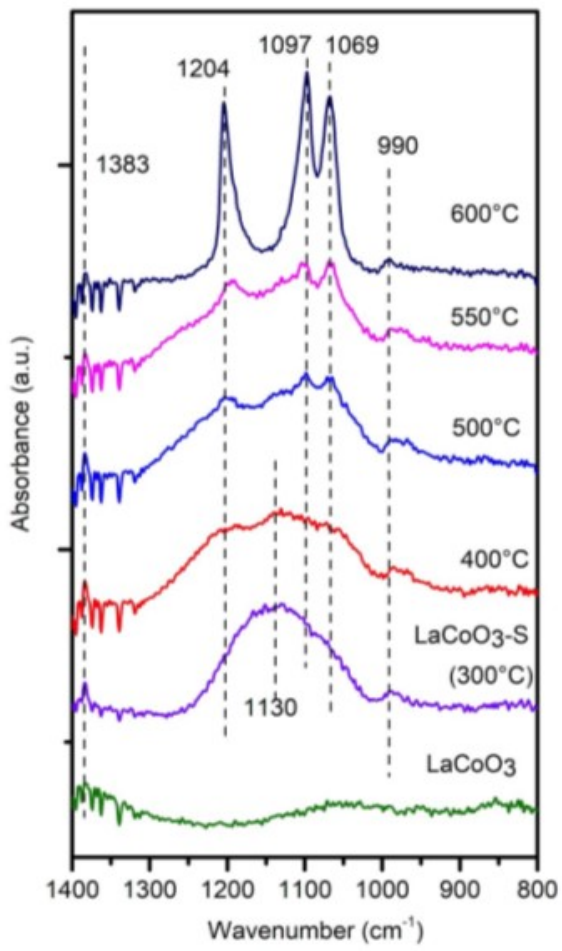

Fig. 4 DRIFT spectra of the LaCoO3 and LaCoO3-S and the thermal evolution of the surface and bulk sulfates. LaCoO3-S is heated to 400, 500, 550 and 600 °C with a hold time of 30 minutes each.

Detailed IR studies during sequential adsorption of NO followed by SO2 showed that the replacement of the nitrites/nitrates was highly dependent of the adsorption mode.11 Namely, at first the nitrates bound to multiple sites (meaning in bridging and bidentate configuration) were replaced while the monodentate nitrate form was the last to be substituted by SO2. This implies that the formation
and dissociation of the NO2 is strongly hindered by the competitive adsorption. While a single free catalytic site is theoretically enough for the NO oxidation reaction to proceed, it is reasonable to expect that catalytic cycle is strongly inhibited when the fraction of the free sites (occupied by $SO4^{2-}$) decreases below a critical value.[25] Between 400 and 600 °C, the characteristic peaks associated with bulk sulphates at the wavenumbers 1069, 1097 and 1204 cm^{-1} are progressively distinguished.[11,20,24] As the temperature increases, the sulphates become more mobile and migrate from the surface into the bulk of the perovskite and occupy energy states that are more favourable. This migration was also confirmed via XPS (see supplementary material Figure S2) and a uniform low concentration of S was observed through the whole depth profile on a LaCoO3-S that was calcined at 600 °C. As will be discussed later in more detail, this increase sulphate mobility is also evident during the soot-TPR (Figure 6). As the sulphates spillover, the

soot consumes one of the oxygen in the sulphate and CO2 and SO2 were simultaneously observed in the gas phase in the corresponding temperature range of 500-600 °C.

Catalytic activity and regeneration

The NO oxidation in the presence of the LaCoO3 catalyst (Figure 5) initiated as low as 200 °C and rapidly increased, reaching very high NO2/NOx ratio (=0.8) and the thermodynamic equilibrium already at 300 °C, even at the high flowrates used in the study. This highlights the potential of LaCoO3 as a low-cost alternative to PGM-based DOC and cDPF. The catalyst was however very sensitive to SO2 (vide infra in Figure 7) and fully deactivated within 90 min. The deactivation was irreversible, and no NO oxidation activity could be recovered after turning off the SO2 flow. The SO2 concentration used in this study was higher than that usually found in the low-sulphur diesel exhausts (5 ppm vs 60 ppm). However, considering that the other parameters such as temperature, space velocity, etc. are similar, this procedure can be reasonably considered an accelerated deactivation giving rise to a calculated SO2 uptake corresponding to ca. 15.000 km of vehicle usage. By considering that a total amount of 6 mmol SO2/gcat passed during 90 minutes of test and we assumed that a vehicle has a fuel consumption of 6 kg/100 km with 10 ppm of S in the fuel (Euro 5 fuel upper limit, EN 590:2009) and a total catalyst load of 200 g is present in the aftertreatment system, the amount of SO2 equivalent to the laboratory test would be reached after ca. 15,000 km. This would imply that during its lifetime the DOC, cDPF etc. would have to be regenerated many times to recover its initial performance. Here, the first regeneration method was washing the catalyst with distilled water. The sulphates, present in small amount and only at the surface, can be easily dissolved and the catalyst activity is fully recovered. This method has been suggested before for the treatment of sulphur poisoned catalysts, including industrial SCR systems.[24,26–28] Even after 5 regeneration cycles, no significant decrease in activity was observed. It should be noted that the same method could be not appropriate for the PGM-based catalysts, as the active component is expensive, and present only at very low (< 1%) amount and could be easily washed away.

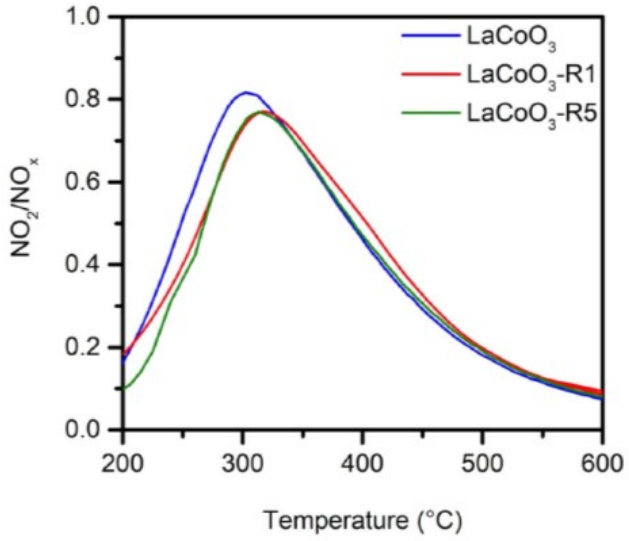

Fig. 5 NO oxidation activity of the fresh and regenerated LaCoO3 samples. Reaction conditions: 200 mg of catalyst, 600 mL min−1 flow rate of 500 ppm NO, 4% O2 in N2, 5 °C min^{-1} heating rate.

The sulphur poisoned catalyst can be regenerated in-situ either by thermal desorption, to which temperatures above 900 °C are required, or at lower temperatures, however above 600 °C, if reducing atmosphere is used (Figure 2 and 6). The extremely high temperatures required for thermal regeneration can irreversibly damage the catalyst, which makes reducing treatment preferable and it is used for the Pt-Ba based LNT applications. Typical reductants for LNT are H2, NH3 and C3H6, with a corresponding increase of the regeneration temperature. Such a procedure not only requires large amount of fuel to be injected during the desulphurization, but also irreversibly damages the catalyst which is

exposed to high temperature and consequent structural changes.[4,9,29,30] To avoid the high fuel penalties associated with the regeneration by the injection of external reductant, soot was demonstrated here, for the first time, to be an efficient SO2 regeneration medium. From the practical point of view, soot is an interesting alternative as it is a pollutant in the diesel exhaust and abundantly available on the cDPF. From the mechanistic point of view, soot is an interesting reacting species as, unlike most heterogeneous reactions which involve solid-gas interface, the soot oxidation involves solid-solid contact. For this reason, the soot-TPR is a good indicator for the differentiation of the highly reactive surface and lattice oxygen and the oxygen spillover rate. In Figure 6, the evolution of the different products during soot-TPR is shown. In contrast to the H2-TPR, where bound sulphur is reduced to H2S before being released in the gas phase, in the case of soot-TPR the bond between $SO4^{2-}$ and LaCoO3-S is broken by releasing the more reactive oxygen in the soot oxidation. The reaction products are indeed SO2 and CO2, whereas almost no CO could be detected, despite oxygen free atmosphere, indicating oxygen spillover (reactions R5-9), in the temperature range between 500-600 °C .The increased sulphate mobility and spillover is also clearly observed during the DRIFTS analysis as the sulphate species rapidly change from surface to bulk sulphate at this temperature (figure 4). The same mechanism occurs during the thermal decomposition as, without soot to accept the active oxygen species, the latter are released first by increasing the temperature before the desorption of SO2, i.e. it is necessary that strongly bound sulphates decompose to sulphites before the SO2 desorption. However, during thermal desorption there is no nearby oxygen acceptor and sulphates decomposition requires more energy. As with H2-TPR, the lattice oxygen species are not available until the sulphur species are removed from the surface. This is evident since with the LaCoO3 catalyst soot oxidation was started at lower temperatures, whereas on LaCoO3-S significant soot oxidation is observed right after SO2 is released (Figure 6).

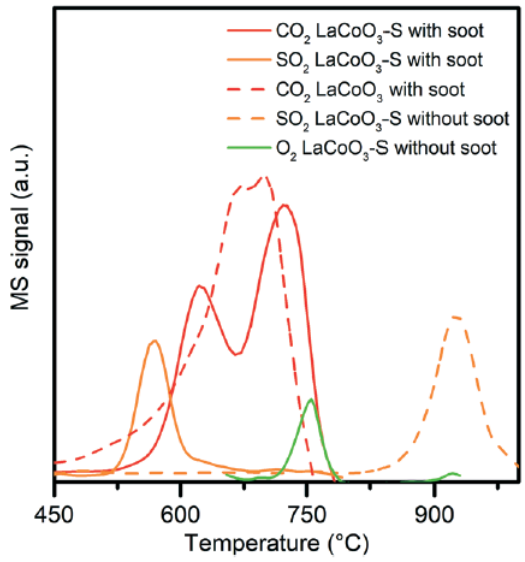

Fig. 6 Soot-TPR and TPD of the LaCoO3 and LaCoO3-S samples. Reaction conditions: 60 mg of catalyst, 60 mL min−1 flow rate of Ar, 5 °C min−1 heating rate. Note that the different product species are not normalized.

As almost all the bound sulphur is released below 600 °C during soot-TPR, the required regeneration temperature is lower than that of H2 regeneration (see figure 2) as well as of thermal decomposition (above 900 °C). At the same time, the complete reduction and the consequent destruction of the perovskite structure is avoided. The reduction of LaCoO3 and LaCoO3-S by soot (R5-R7) and the thermal decomposition and desorption of sulphates (R8-R9) occur according to the following reactions:

(R4) LaCoO3-SO3 + C → LaCoO3 + SO2 + CO2 R5 (500-600 °C)
(R5) 4 LaCoO3 + C → 4 LaCoO2.5 + CO2 R6 (550-700 °C)
(R6) 2 LaCoO2.5 + C → Co/La2O3 + CO2 R7 (600-800 °C)
(R7) LaCoO3-SO3 → LaCoO3-SO2 + O2 R8 (700-800 °C)
(R8) LaCoO3-SO2 → LaCoO3 + SO2 R9 (850-1000 °C)

The temperature required for the soot-mediated sulphate removal is higher (> 500 °C from R5) than that typically encountered in the diesel engine exhaust during normal operation of the diesel engine. However, both the soot buildup and SO2 poisoning have a complementary tendency over the cDPF. In fact, during normal operation the produced NO2 oxidizes the soot continuously thus enabling passive regeneration of the filter. As the catalyst is poisoned by SO2, the NO2 production falls down and thereby the soot builds up on the catalysed filter, that starts to behave as a non-catalysed filter. Once the backpressure is high, fuel injection is required to achieve high temperature and to burn off the accumulated soot. The soot-assisted regeneration is not expected to operate passively, but it could enable lower regeneration temperature with lower amount of additional fuel required. The last phenomenon explored here is not regeneration, but deactivation prevention (Figure 7).

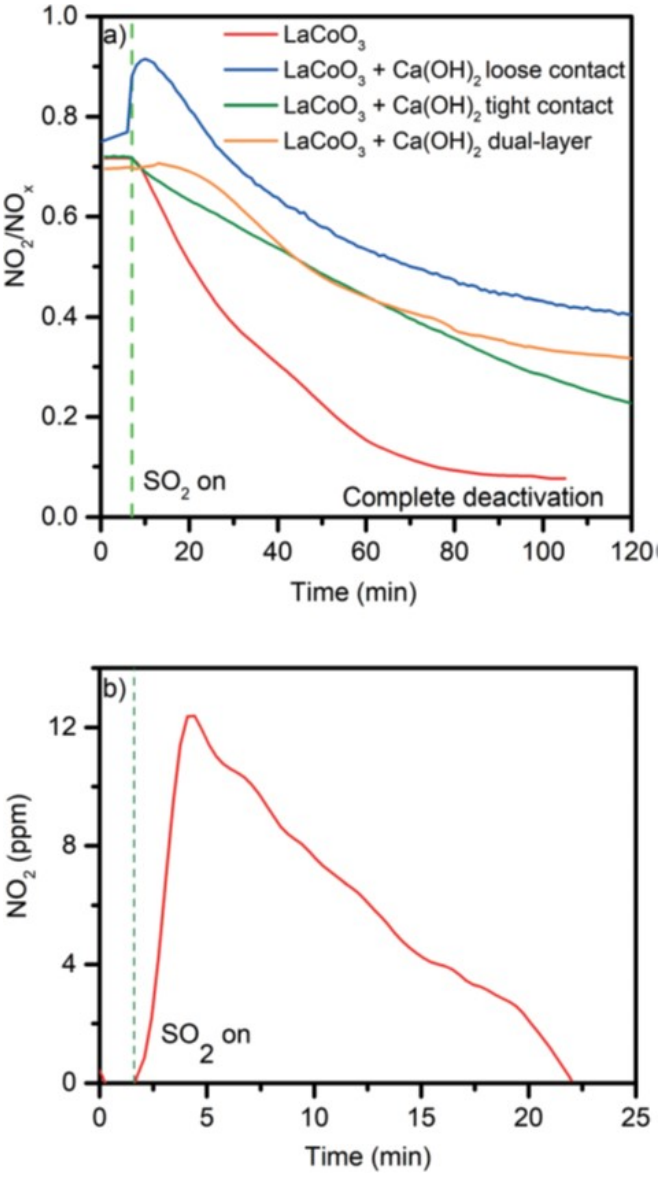

Fig. 7 a) Deactivation of LaCoO3 as pure and mixed with Ca)OH)2. Reaction conditions: 200 mg catalyst, 100 mg CaIJOH)2, 600 mL min^{-1} 500 ppm NO, 4% O2, in N2 and 60 ppm SO2 when added, T = 300 °C. b) The competitive adsorption of SO2 on LaCoO3 pre-saturated with NOx, reaction conditions same as before, T = 200 °C.

The LaCoO3 sample was physically mixed with small amounts of Ca(OH)2, an alkaline compound apt to SO2 capture. Increasing the basicity of the perovskite by doping during synthesis with Sr was shown to increase its resistance to SO2 poisoning, by capturing the sulphates during the poisoning. The approach used here was slightly different, in the sense that the basic compound was added post synthesis. Three configurations were compared, whereby the contact between the catalyst and adsorbent was varied. The LaCoO3 mixed with Ca(OH)2 both in tight contact and in dual-layer enhanced the resistance to poisoning, however the best performance was obtained by the loose contact configuration, confirming that Ca(OH)2 was more efficient in capturing SO3 than SO2. The poisoning was also repeated at 500 °C and the same trends were observed. The adsorbent was also effective at a higher temperature, the only difference being that at 500 °C a longer time was required to reach complete deactivation of the catalyst with respect to poisoning at 300 °C (Fig. S3†).

When SO2 was in contact with the (LaCoO3 + Ca(OH)2) physical mixture a temporary evolution of NO2 was observed, as SO3 substituted the previously adsorbed NO2 according to reactions (R9)–(R11). The initial deactivation rate was fast since Ca(OH)2 mainly adsorbed the oxidized form of Sox ((R7)–(R9)). After the initial deactivation stage, the catalyst maintained a stable ca. 50% initial activity for a prolonged time. Even after 6 hours of poisoning, a further decrease in the activity was negligible. This method could offer an inexpensive and simple method for the delay and mitigation of deactivation.

(R9) $Ca(OH)_2 + SO_3 \rightarrow CaSO_4 + H_2O$
(R10) $Ca(OH)_2 + 2NO_2 \rightarrow Ca(NO_3)_2 + H_2O$
(R11) $2Ca(NO_3)_2 + 2SO_3 \rightarrow 2CaSO_4 + 5NO_2$

The two-phase competitive deactivation was demonstrated more clearly (Fig. 7b) on pure LaCoO3, which was saturated with NOx before switching off the NOx flow and turning on SO2. A clear evolution of NO2 was observed upon SO2 introduction, as the previously adsorbed NO2 was being replaced by the SO3 species having higher affinity during the competitive adsorption for the same catalytic active sites. The timespan of this substitution, ca. 20 minutes, corresponded to the timespan of the initial fast deactivation phase.

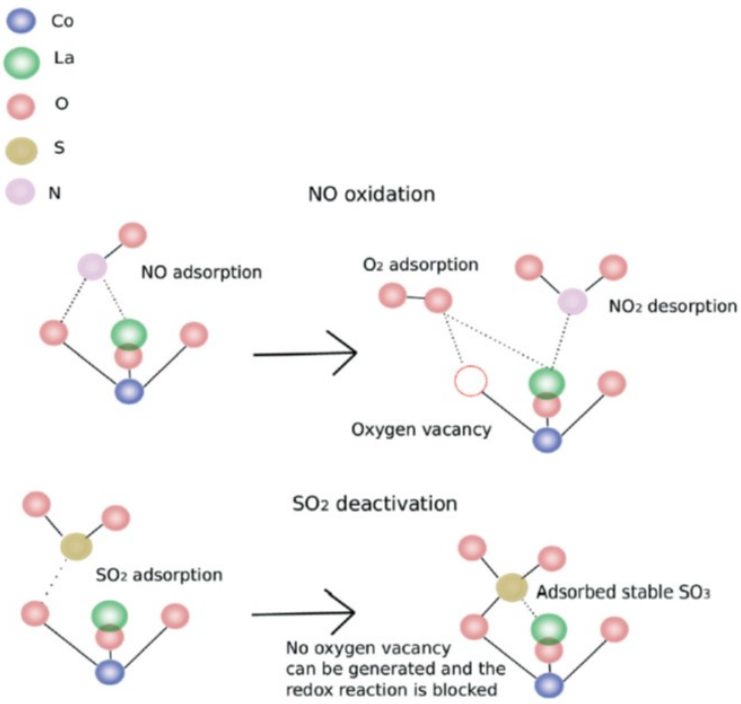

Conclusions

The deactivation of LaCoO3 by SO2 was investigated under reaction conditions relevant to diesel aftertreatment systems. Although LaCoO3 had excellent NO oxidation activity, it rapidly deactivated in the presence of SO2. Investigation of the deactivated sample by XPS showed that sulphur existed as sulphate species only at the surface, bound to lanthanum rather than to cobalt. As confirmed by DRIFTS and soot-TPR, sulphate mobility and diffusion into the bulk of the perovskite or spillover to soot started only above 500 °C and completed at 600 °C. The bound sulphates blocked gradually the active sites required for NO oxidation. After the initial fast deactivation, which can be ascribed to active site blocking, a second (slower) stage followed, during which multilayered lanthanum sulphates formed at the surface of the catalyst following the deactivation scheme proposed in Fig. 8. The reported activity tests and characterization of the catalyst suggest a two-stage deactivation mechanism: a fast (initial) stage where deactivation occurs by competitive adsorption and chemical blocking of the active sites by sulphates, followed by a second (slower) stage where multilayer lanthanum sulphate forms on the catalyst surface

physically blocking the sites.[18,30] Reactivity studies showed that the basic and redox sites on the catalyst were blocked by $SO4^{2-}$, and for them to be reactivated, the strongly bound sulphur species had to be removed. Washing with water effectively removed the surface sulphates and the reactivated catalyst regained nearly the initial activity, even after 5 poisoning/regeneration cycles. Mixing small amounts of Ca(OH)2 as an adsorbent delayed the complete deactivation and the catalyst retained nearly half of its initial activity for extended period. This method proved, however, ineffective in completely preventing the initial "fast" stage of the deactivation. Finally, soot was explored as a potential regenerating agent, since one of the main potential uses of LaCoO3 would be in catalysed diesel particulate filters. The soot acted as an oxygen acceptor from the surface sulphate and effectively released sulphur as SO2 below 600 °C, a temperature lower than that required for H2 mediated desulphurization.

Acknowledgements
This work was funded through a SINCHEM Grant. SINCHEM is a Joint Doctorate programme selected under the Erasmus Mundus Action 1 Programme (FPA 2013-0037).

References
1 J. Zhu, H. Li, L. Zhong, P. Xiao, X. Xu, X. Yang, Z. Zhao and J. Li, ACS Catal., 2014, 4, 2917–2940.
2 C. Zhou, Z. Feng, Y. Zhang, L. Hu, R. Chen, B. Shan, H. Yin, W. G. Wang and A. Huang, RSC Adv., 2015, 5, 28054–28059.
3 R. You, Y. Zhang, D. Liu, M. Meng, L. Zheng, J. Zhang and T. Hu, J. Phys. Chem. C, 2014, 118, 25403–25420.
4 X. He, J. He and M. Meng, Catal. Lett., 2011, 141, 1364–1370.
5 H. Wang, Z. Zhao, P. Liang, C. Xu, A. Duan, G. Jiang, J. Xu and J. Liu, Catal. Lett., 2008, 124, 91–99.
6 D. Fino, S. Bensaid, M. Piumetti and N. Russo, Appl. Catal., A, 2016, 509, 75–96.
7 L. Yang, G. Li, G. Gao, R. Xu, S. Zhu, X. Shu, S. Wang, Z. Deng and P. Wang, RSC Adv., 2017, 7, 52352–52356.
8 A. Amberntsson, M. Skoglundh, S. Ljungström and E. Fridell, J. Catal., 2003, 217, 253–263.
9 D. H. Kim, A. Yezerets, J. Li, N. Currier, H. Y. Chen, H. Hess, M. H. Engelhard, G. G. Muntean and C. H. F. Peden, Catal. Today, 2012, 197, 3–8.
10 D. H. Kim, J. H. Kwak, J. Szanyi, X. Wang, G. Li, J. C. Hanson and C. H. F. Peden, J. Phys. Chem. C, 2009, 113, 21123–21129.
11 M. Kurt, Z. Say, K. E. Ercan, E. I. Vovk, C. H. Kim and E. Ozensoy, Top. Catal., 2017, 60, 40–51.
12 H. Xian, F. L. Li, X. G. Li, X. W. Zhang, M. Meng, T. Y. Zhang and N. Tsubaki, Fuel Process. Technol., 2011, 92, 1718–1724.
13 H. Wang, Y. Zhu, R. Tan and W. Yao, Catal. Lett., 2002, 82, 199–204.
14 A. Kumar, M. P. Harold and V. Balakotaiah, J. Catal., 2010, 270, 214–223.
15 S. Royer, A. Van Neste, R. Davidson, B. McIntyre and S. Kaliaguine, Ind. Eng. Chem. Res., 2004, 43, 5670–5680.
16 Y. Zhu, R. Tan, J. Feng, S. Ji and L. Cao, Appl. Catal., A, 2001, 209, 71–77.
17 S. Hodjati, C. Petit, V. Pitchon and A. Kiennemann, Appl. Catal., B, 2001, 30, 247–257.
18 O. Buchneva, I. Rossetti, C. Biffi, M. Allieta, A. Kryukov and N. Lebedeva, Appl. Catal., A, 2009, 370, 24–33.
19 I. Rossetti, O. Buchneva, C. Biffi and R. Rizza, Appl. Catal., B, 2009, 89, 383–390.
20 R. Zhang, H. Alamdari and S. Kaliaguine, Appl. Catal., A, 2008, 340, 140–151.
21 Q. N. Tran, F. Martinovic, M. Ceretti, S. Esposito, B. Bonelli, W. Paulus, F. Di Renzo, F. A. Deorsola, S. Bensaid and R. Pirone, Appl. Catal., A, 2020, 589, 117304.
22 B. M. Abu-Zied, S. M. Bawaked, S. A. Kosa and W. Schwieger, J. Nanomater., 2015, 580582.
23 D. Briggs, Handbook of X-ray Photoelectron Spectroscopy, ed. C. D. Wanger, W. M. Riggs, L. E. Davis, J. F. Moulder and G. E. Muilenberg, Perkin-Elmer Corp., Physical Electronics Division, Eden Prairie, Minnesota, USA, 1979, 190 pp. $195, 1981, vol. 3.
24 I. Rosso, G. Saracco and V. Specchia, Korean J. Chem. Eng., 2003, 20, 222–229.
25 C. Barroo, V. Voorsluijs, T. Visart De Bocarmé, P. Gaspard and Y. De Decker, Phys. Chem. Chem. Phys., 2018, 20, 21302–21312.
26 X. Shang, G. Hu, C. He, J. Zhao, F. Zhang, Y. Xu, Y. Zhang, J. Li and J. Chen, J. Ind. Eng. Chem., 2012, 18, 513–519.

27 Y. Yu, C. He, J. Chen, L. Yin, T. Qiu and X. Meng, Catal. Commun., 2013, 39, 78–81.
28 Y. Wang, D. Ge, M. Chen, S. Gao and Z. Wu, Catal. Commun., 2018, 117, 69–73.
29 J. McCarthy and J. Holtgreven, in SAE Technical Papers, 2008, 2008-01-1541.
30 P. Lott, M. Eck, D. E. Doronkin, R. Popescu, M. Casapu, J. D. Grunwaldt and O. Deutschmann, Top. Catal., 2019, 62, 164–171.